Probing Molecular Structures of Polymer/Metal Interfaces by Sum Frequency Generation Vibrational Spectroscopy

Xiaolin Lu,[†,‡] Nick Shephard,[§] Jianglong Han,[‡] Gi Xue,[‡] and Zhan Chen*[,†]

Department of Chemistry, University of Michigan, 930 North University Avenue, Ann Arbor, Michigan, 48109, Department of Polymer Science, Nanjing University, Nanjing, People's Republic of China, 210093, and ATVB Business, Materials Science Technology Platform, Dow Corning Corporation, 2200 W. Salzburg Road, Midland, Michigan, 48686

Received July 24, 2008; Revised Manuscript Received September 21, 2008

ABSTRACT: Sum frequency generation (SFG) vibrational spectroscopy has been applied to investigate the molecular structure of the buried poly(methyl methacrylate) (PMMA)/silver (Ag) interface. To elucidate such a structure, PMMA films with different thicknesses deposited on Ag substrates have been studied in the experiments. SFG signals collected from such PMMA films are interference results of the signals generated from the PMMA/air and PMMA/Ag interfaces. Such signals also include some nonresonant contributions from the samples. When the PMMA film thickness is changed, such an interference effect also varies. SFG signals from the buried PMMA/Ag interface have been successfully deconvoluted from such detected interference results, from which molecular structure of the PMMA/Ag interface can be inferred. The signals from the ester methyl groups dominate the SFG signals deduced for the PMMA/Ag interface, indicating the dominating presence of the ester methyl groups at this interface. The ester methyl groups point away from the Ag surface with a large tilt angle. They lie down more toward the interface compared to those on the PMMA surface in air. Methylene and α-methyl groups are also detected at the PMMA/Ag interface. This research demonstrates that SFG is a viable technique to elucidate molecular structures of buried polymer/metal interfaces.

1. Introduction

Interfacial properties such as adhesion are controlled by molecular interfacial structures. Understanding molecular structures of organic materials (such as polymers) at an interface with metal is crucial for the development of adhesives in microelectronic assembly, paints, coatings, composites, and anticorrosives.[1] However, such interfaces are buried and thus it is difficult to probe their structures using conventional analytical techniques. Traditionally, to study such structures, the buried interfaces need to be broken, and the two resulting surfaces exposed to air can be investigated.[2,3] Important structural information has been deduced from such studies. Sometimes such experimental procedures may alter the interfacial structures, especially for those interfaces which have good adhesive properties. Therefore, it is necessary to develop a technique which can probe molecular structures of buried interfaces *in situ*. In this research, we want to develop methods to probe polymer/metal interfacial structures at the molecular level *in situ*.

Recently, sum frequency generation (SFG) vibrational spectroscopy has been applied to study molecular structures of surfaces and interfaces, including polymer surfaces.[4−38] SFG is a nonlinear optical vibrational spectroscopic technique which can selectively probe molecular structure of a surface or an interface with a submonolayer surface specificity *in situ*.[4−38] It has been used to study many interfacial problems involving polymers,[4−38] such as polymer surface structures in air, polymer surface restructuring in water, molecular interactions between polymer surfaces and biomolecules (such as proteins), polymer/polymer interfaces, and surface structures of polymer blends and copolymers. Here we select the poly (methyl methacrylate) (PMMA)/silver (Ag) system as a model to study polymer/metal interfaces using SFG.

PMMA is widely used as materials for biomedical implants, barriers, membranes, micro lithography, and optical applications.[39−43] In all these applications, understanding surface/interfacial structures of PMMA is very important. PMMA surfaces have been extensively studied by many research groups using various techniques including surface tension measurements, secondary ion mass spectrometry (SIMS), and X-ray photoelectron spectroscopy (XPS). Excellent results have been obtained from such studies.[44−52]

Surface structures of PMMA have also been investigated using SFG in our group.[12,13] It was found that in air the ester methyl groups dominate the surface. Such ester methyl groups more or less stand up on the surface. Weak carbonyl SFG signals have been detected, showing some presence of carbonyl groups on the PMMA surface in air. Research also shows that different from surface dominating methyl groups of other polymethacrylates with longer side chains, ester methyl groups on the PMMA surface do not restructure in water.[13] This may be due to the fact that they are more hydrophilic than normal methyl groups, and PMMA structure is quite rigid. The surface structures of PMMA in air as a function of temperature were studied by Chou et al. using SFG.[35] The surface structural changes of PMMA after the deposition of a layer of SiO_2 has also been examined using SFG by Miyamae and Nozoye.[38] In addition to the pure PMMA polymer, PMMA polymer blends and copolymers with other polymers have been investigated using SFG in our group as well as other laboratories.[23,37] In this study, SFG has been applied to investigate the molecular structure of the buried PMMA/Ag interface. SFG spectra of PMMA films with different thicknesses on Ag have been collected and analyzed. Such spectra are the result of interference between those contributed from the PMMA/air interface and the PMMA/Ag interface. An existing model published in the literature[53] has been adopted to analyze such spectra to deconvolute the SFG signal generated from the PMMA/Ag interface, from which structural information of the polymer/metal interface can be deduced. We believe that

* To whom all correspondence should be addressed. E-mail: zhanc@umich.edu. Fax: 734-647-4685.
[†] Department of Chemistry, University of Michigan.
[‡] Department of Polymer Science, Nanjing University.
[§] ATVB Business, Materials Science Technology Platform, Dow Corning Corporation.

10.1021/ma801680f CCC: $40.75
Published on Web 10/28/2008

the methodology presented in this research is general, which can be applied to study many other polymer/metal interfaces *in situ* at the molecular level using SFG in the future. We should mention that excellent research applying SFG to study organic molecules at buried interfaces and other buried polymer interfaces (but not polymer/metal interfaces) through investigating polymer films with different thicknesses has been published previously.[29,30,54,55]

2. Experimental Section

2.1. Materials. PMMA has been purchased from Sigma-Aldrich Co. with M_w of 996 000 (GPC data from the company). PMMA films were prepared by spin-coating PMMA solution in toluene onto the substrates. The PMMA film thickness was controlled by adjusting the spin speed and the solution concentration. Two types of substrates, fused silica windows and evaporated silver layer on glass, were used in this research. Fused silica windows were purchased from Esco Products, Inc. They were pretreated by a sulfuric acid bath saturated with potassium dichromate and air plasma to remove the possible surface contamination before spin-coating. Silver substrates were prepared by depositing a 500-nm silver layer on glass slides (with a 15-nm nickel layer in between to promote the adhesion) using an electron-beam evaporator (Cooke Evaporator, Cooke Vacuum Products). The glass slides were pretreated by piranha solution (a mixed solution with 3:7 volume ratio of 30 wt % H_2O_2 solution and 98 wt % H_2SO_4) to eliminate the possible surface contamination. The prepared PMMA samples on substrates were placed in a vacuum dessiciator overnight. The PMMA film thicknesses were measured by an ellipsometer (EP3-SW imaging ellipsometer, Nanofilm Technologie, GmbH). SFG spectra were collected with the face-down geometry (with the input laser beams going through the substrate and the PMMA film to reach the PMMA/air interface)[15] for the samples on the fused silica window and with the face-up geometry (with the input laser beams directly reaching the PMMA samples from air)[12] for the samples on the Ag substrates.

2.2. SFG Experiment. SFG theory has been well developed and extensively published in the literature.[56−66] The SFG setup and experimental geometry used in the current investigation have been reported in previous publications.[12−24] Briefly, the visible and infrared (IR) input beams overlap spatially and temporally on the polymer surface with input angles of 60° and 54° respectively and beam diameters of approximately 500 μm. The pulse energies of the visible and IR beams were approximately 3 μJ and 90 μJ respectively for PMMA films on Ag. The lower pulse energies were used to avoid burning the samples.

In the current investigation, the spectra were taken in the ssp (s-polarized sum frequency output, s-polarized visible input, and p-polarized IR input) and sps polarization combinations. For the PMMA films on the fused silica substrates, both ssp and sps SFG spectra in the frequency range between 2800 and 3100 cm^{-1} were detected. For the PMMA films on Ag substrates, in the same frequency range, only ssp SFG spectra were collected.

3. SFG Data Analysis

The SFG output intensity in the reflected direction can be written as[66]

$$I(\omega) = \frac{8\pi^3\omega^2 \sec^2\beta}{c^3 n_1(\omega) n_1(\omega_1) n_1(\omega_2)} \left|\chi_{eff}^{(2)}\right|^2 I_1(\omega_1) I_2(\omega_2) AT \qquad (1)$$

where $n_1(\omega_i)$ is the refractive index of the incident medium at frequency ω_i, ω, and β are the frequency and the reflection angle of the sum frequency field, respectively. $I_1(\omega_1)$ and $I_2(\omega_2)$ are the intensities of the two input fields with frequencies ω_1 and ω_2. T is the pulse-width of both input lasers. A is the overlapping cross section of the two input beams at the sample, and $\chi_{eff}^{(2)}$ is the effective second-order nonlinear optical susceptibility. The different tensor components of $\chi^{(2)}$ ($\chi^{(2)}$ is the second-order nonlinear optical susceptibility defined in the laboratory-fixed coordination system) can be measured through collecting SFG spectra using certain different polarization combinations.[66] For example,

$$\chi_{eff,ssp}^{(2)} = L_{yy}(\omega) L_{yy}(\omega_1) L_{zz}(\omega_2) \sin\beta_2 \chi_{yyz} \qquad (2)$$

$$\chi_{eff,sps}^{(2)} = L_{yy}(\omega) L_{zz}(\omega_1) L_{yy}(\omega_2) \sin\beta_1 \chi_{yzy} \qquad (3)$$

Here χ_{yyz} and χ_{yzy} are different components of $\chi^{(2)}$ with the lab coordinates chosen such that z is along the interface normal and x is in the input laser incident plane. $\chi_{eff,ssp}^{(2)}$ and $\chi_{eff,sps}^{(2)}$ are the components of the effective second-order nonlinear optical susceptibility measured in the experiment by collecting the ssp and sps SFG spectra. L_{ii}'s (i = x, y, or z) are the Fresnel coefficients, and β_1 and β_2 are angles between the surface normal and the input visible beam, and the input IR beam, respectively. When the IR frequency is near the vibrational resonance, the effective second-order nonlinear susceptibility can be written as (using ssp polarization combination as an example):

$$\chi_{eff,ssp}^{(2)} = \chi_{NR} + F_{sur} \sum_q \frac{A_q}{\omega_2 - \omega_q + i\Gamma_q} \qquad (4)$$

$$F_{sur} = L_{yy}(\omega) L_{yy}(\omega_1) L_{zz}(\omega_2) \sin\beta_2 \qquad (5)$$

χ_{NR} is the nonresonant background. F_{sur} is the complex Fresnel coefficient and its value can be obtained from eq 5. A_q, ω_q, and Γ_q are the strength, resonant frequency, and damping coefficient of the vibrational mode q. The SFG spectra from a surface or an interface can then be fitted using Equation 6:

$$I(\omega) = C\left|\chi_{NR} + F_{sur} \sum_q \frac{A_q}{\omega_2 - \omega_q + i\Gamma_q}\right|^2 \qquad (6)$$

Clearly, A_q, ω_q, and Γ_q can be obtained by fitting the SFG spectra. C is the proportional factor.

4. Results and Discussions

4.1. Summary of the PMMA/Air Interface Structural Studies. Previously, the molecular surface structure of PMMA in air has been studied in detail using SFG in our laboratory.[12] We used a PMMA film deposited on a fused silica substrate to study the PMMA/air interface in that research. It was shown that SFG signals collected from such a sample are contributed by the PMMA/air interface, with almost no contribution from the PMMA/fused silica interface or the PMMA bulk.[12] The PMMA/air interface is dominated by the ester methyl groups. Such surface dominating ester methyl groups on the PMMA surface in air have some orientation ordering. From ssp, ppp, and sps SFG spectra, we deduced that the orientation and orientation distribution of ester methyl groups assuming a Gaussian distribution $f(\theta) = C \exp[-(\theta - \theta_0)/2\sigma^2]$. Here θ_0 and σ are defined as average orientation angle and orientation angle distribution. The results indicated that the orientation and orientation distribution of ester methyl groups should be between the orientation angle θ_0 of 33° vs the surface normal with a δ angle distribution ($\sigma = 0$) and θ_0 of 0° vs the surface normal with an angle distribution σ of 31°, assuming a Gaussian orientation distribution. The measured SFG intensity calibrated by a z-cut quartz confirms this conclusion. We also find that the α-methyl groups tend to lie down on the PMMA surface, and the methylene groups are not detected on the PMMA surface in air.

In order to reliably deconvolute SFG signals generated from the buried PMMA/Ag interface from the SFG signals collected from the PMMA films on Ag which contain both contributions from the PMMA/air interface and the PMMA/Ag interface, it is necessary to use the "known" SFG signals generated from the PMMA/air interface. We therefore collected SFG spectra

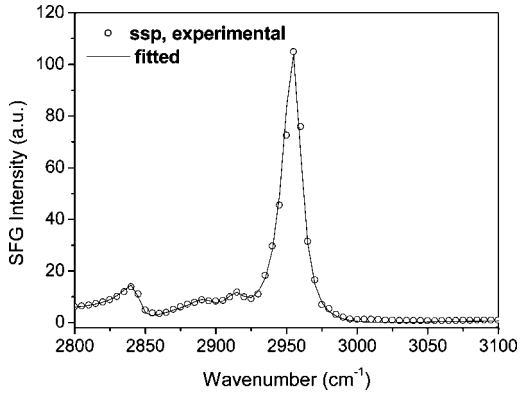

Figure 1. The ssp SFG spectrum from a 44-nm PMMA film on a fused silica window.

Table 1. Fitting Results for the SFG Spectra of the PMMA Surface in Air and the PMMA Interface with the Ag Substrate (Fresnel Coefficients Are Included into the Fitting)

	A_i (ssp)		
ω_i (cm^{-1})	PMMA surface in air	PMMA interface with the Ag substrate	Γ_i
2844	28.0	150.0	7.0
2895	12.0	0	9.0
2918	15.0	0	8.0
2940	−5.0	−180.0	7.0
2955	138.0	260.0	8.0
2991	0	−80.0	11.0
3020	0	−65.0	11.0

again from the PMMA films deposited on fused silica substrates and carefully fit such spectra in this research. The ssp SFG spectrum collected from the PMMA/air interface is shown in Figure 1 and the fitting results are displayed in Table 1. The SFG spectrum and the fitting results are quite similar to the results we published previously.[12]

The peak assignments for vibrational signals of PMMA have been discussed several times in the published results[67−71] and also in our previous paper.[12] It is believed that the ~3020 cm^{-1} peak is from one of the C−H asymmetric stretching mode of the ester methyl group. The ~2990 cm^{-1} peak is contributed from another C−H asymmetric stretching mode of the ester methyl group, as well as a C−H asymmetric stretching mode of the α-methyl group. The ~2955 cm^{-1} signal in the ssp spectra is mainly contributed by the C−H symmetric stretching mode from the ester methyl group. The infrared spectroscopic studies on isotope labeled PMMA indicate that the peak around 2930 to 2940 cm^{-1} is contributed by the C−H symmetric stretching of the α-methyl and methylene groups.[67−71]

We also collected the sps spectrum from the PMMA/air interface (not shown). Like the ssp spectrum, it is also similar to what was published before.[12] This research reproduced the experimental results which we published previously. The ssp results will be used in the data analysis below to deduce the SFG signals from the PMMA/Ag interface.

4.2. PMMA/Ag Interface. *4.2.1. Fitting the SFG Spectra of the PMMA Films on the Ag Substrates.* Now considering a PMMA film on a silver substrate, the inversion symmetry is broken at both the PMMA/air interface and the PMMA/Ag interface so that both interfaces can generate resonant SFG signals. SFG signals collected from the PMMA films should be interference results from the signals contributed by these two interfaces. Similar interference results have been observed in previous publications.[29,30] The effective second-order nonlinear susceptibility can thus be written as:

$$\chi^{(2)}_{eff,ssp} = L_{yy}^{surface}(\omega)L_{yy}^{surface}(\omega_1)L_{zz}^{surface}(\omega_2)\sin\beta_2\chi_{yyz}^{surface} + L_{yy}^{interface}(\omega)L_{yy}^{interface}(\omega_1)L_{zz}^{interface}(\omega_2)\sin\beta_2\chi_{yyz}^{interface} + \chi_{NR}e^{i\varphi_{ssp}} \quad (7)$$

$L_{ii}^{surface}$ and $L_{ii}^{interface}$ ($i = x$, y, or z) are the Fresnel coefficients of the PMMA/air interface and the PMMA/Ag interface, respectively. $\chi_{yyz}^{surface}$ and $\chi_{yyz}^{interface}$ are the $\chi^{(2)}$ components of the PMMA/air interface and the buried PMMA/Ag interface. χ_{NR} is the nonresonant background signal contributed from the samples, possibly from the Ag substrate, the PMMA bulk film, or various interfaces. Clearly, if $\chi_{yyz}^{surface}$ is known, it would be much easier to deduce $\chi_{yyz}^{interface}$. Various terms in $\chi_{yyz}^{interface}$and χ_{NR} can be obtained by fitting the collected SFG spectra. In order to simplify eq 7, we have

$$F_{yyz}^{surface} = \left|L_{yy}^{surface}(\omega)L_{yy}^{surface}(\omega_1)L_{zz}^{surface}(\omega_2)\sin\beta_2\right| \quad (8)$$

$$F_{yyz}^{interface} = \left|L_{yy}^{interface}(\omega)L_{yy}^{interface}(\omega_1)L_{zz}^{interface}(\omega_2)\sin\beta_2\right| \quad (9)$$

Combining eqs 1, 7, 8, and 9 we then have

$$I(\omega) = C\left|F_{yyz}^{surface}\chi_{yyz}^{surface}e^{i\phi} + F_{yyz}^{interface}\chi_{yyz}^{interface} + \chi_{NR}e^{i\varphi}\right|^2 \quad (10)$$

φ and ϕ are the phase difference between the surface and the interface signal and the phase difference between the nonresonant background and the interface signal, respectively. Equation 10 is the final expression which will be used to fit the ssp SFG spectra generated from the air/PMMA/Ag samples.

4.2.2. Molecular Information of the PMMA/Ag Interface. As discussed, molecular structural information of the buried PMMA/Ag interface can be deduced from SFG spectra collected from the air/PMMA/Ag samples, which contain the spectral contribution from this interface. To accomplish this, SFG spectra from the PMMA films with different thicknesses on the Ag substrates were collected. As shown in the previous publication,[12] the bulk contribution to the SFG signal from the PMMA film is negligible. Therefore, such SFG signals are interference results of spectral contributions from the PMMA/air interface, the buried PMMA/Ag interface, and the nonresonant background. To deduce the SFG signal from the PMMA/Ag interface, the collected SFG spectra were fitted by using eq 10.

First, it is necessary to calculate the Fresnel coefficients of the PMMA/air interface and the PMMA/Ag interface (please see the Supporting Information for more details).[53,72] Figure 2 shows the Fresnel coefficients of the PMMA/air interface, the PMMA/Ag interface, and the phase difference between the PMMA/air interface and the PMMA/Ag interface in terms of the PMMA film thickness. Clearly, such factors vary for each interface when the film thickness is altered, leading to different constructive or destructive signal interferences of the two interfaces as well as the nonresonant background. This should result in substantial variations of the SFG signal intensity when the PMMA films with different film thicknesses are studied.

Figure 3 shows SFG spectra collected from PMMA films on the Ag substrates with different thicknesses of 39, 92, 125, 185, and 247 nm. Indeed SFG spectra intensities are markedly different. It is difficult to fit such thickness dependent SFG spectra well by only using the PMMA/air interface contribution. Figure 4 shows the best fitting results using only the contributions from PMMA in air. They do not match the experimental data very well. We believe that SFG spectra collected from PMMA on the Ag substrates are contributed from both the PMMA/air and PMMA/Ag interfaces. Thus to fit these spectra better, the contributions from both the PMMA/air and the PMMA/Ag interfaces should be included in the fitting using Equation 10.

Figure 5 displays the fitting results when the buried PMMA/Ag interface signal contribution is also considered. Such results

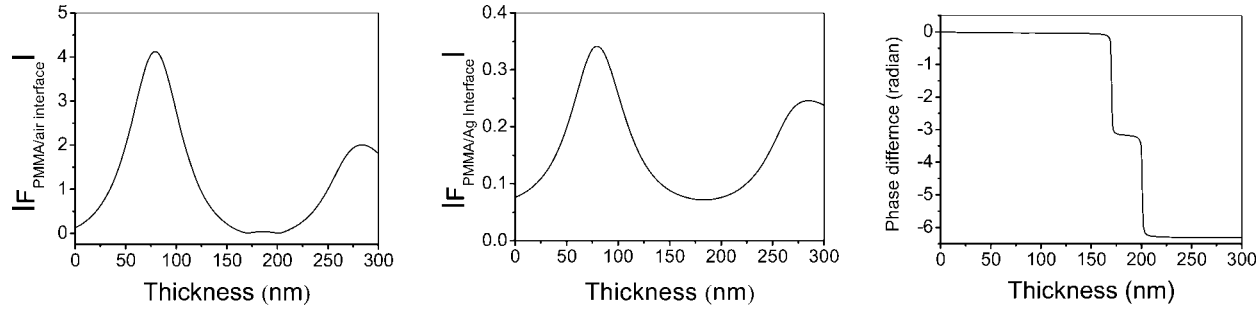

Figure 2. Fresnel coefficients of the PMMA/air interface, the PMMA/Ag interface and the phase difference between the PMMA/air interface and the PMMA/Ag interface in terms of the film thickness.

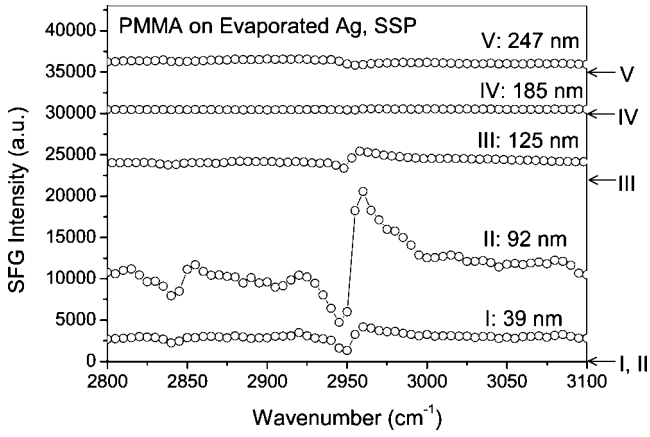

Figure 3. The ssp SFG spectra of PMMA films with different thicknesses on the silver substrates. The arrows on the right indicate the baseline for each spectrum.

can match the experimentally collected SFG spectra very well. Such fittings used contributions from the PMMA/air interface deduced from section 4.1, experimentally measured PMMA film thickness, and signals from the PMMA/Ag interface with a nonresonanct background. We believe that such fittings are reliable because they fit a huge intensity difference among signals from various PMMA samples excellently, and also for almost all the details in various spectral features. Such fittings are much closer to the measured data than those using only the contributions from the PMMA surface in air. The fittings are not only working for a single spectrum, but for all the five spectra collected from the PMMA films with different thicknesses simultaneously.

From such "global" fitting results, the SFG spectrum contributed from the PMMA/Ag interface has been deduced, as shown in Figure 6. The fitting parameters for both the PMMA/air and PMMA/Ag interfaces are shown in Table 1 with the consideration of the Fresnel coefficients. The deduced SFG spectrum from the PMMA/Ag interface is markedly different from that of the PMMA surface in air. In addition to a dominating peak at 2955 cm^{-1}, which is mainly contributed from the C−H symmetric stretching mode of the ester methyl group, a strong peak at 2940 cm^{-1}, a peak with intermediate intensity at 2844 cm^{-1}, two weak peaks at 2991 and 3020 cm^{-1} were also obtained from fitting. We should mention that the fittings for all the peaks are according to equation 10, except that we need to adopt a "special" phase for the 2844 cm^{-1} peak from the PMMA/Ag interface to ensure the good fitting around this frequency. We cannot simply use a "+" or "−" for the signal strength to fit this peak, instead, we need to use an intermediate phase. This is quite a persuasive proof that this peak is not from a single vibrational mode for PMMA. As we will show in more detail later, the peak at 2940 cm^{-1} should be assigned to the methylene symmetric stretch. The negative amplitude of this peak indicates that the methylene groups point to the opposite direction at the interface comparing to the ester methyl groups.

Bain et al. discussed the surfactant adsorbed at a solid surface in a published article.[73] The resonant nonlinear second-order susceptibility changes the sign when the adsorbent changes the absolute orientation, e.g., switches from the "pointing-away from" to the "pointing-to towards" the substrate surface. A relatively large nonresonant background can be used to differentiate the two different absolute orientations since the interference of the nonresonant background and the resonant signal provides the phase information.[73] We also adopted a similar method to determine the absolute orientations of silane molecules at the polymer/silane interfaces.[22] The strongest peak in the deduced SFG spectrum from the PMMA/Ag interface is still the ester methyl symmetric stretch. The signal strength of this peak has the same sign (+260) as that in the SFG spectrum collected from the PMMA/air interface (+138). We believe that the same sign of this peak for the PMMA/air interface and the PMMA/Ag interface indicates that both the ester methyl groups at the PMMA/air interface and the PMMA/Ag interface point to the same direction. We believe that the ester methyl groups on the PMMA surface in air should point to the air, because methyl groups are hydrophobic groups and air is hydrophobic too. Therefore, it can be deduced that the ester methyl groups at the PMMA/Ag interface point away from the Ag substrate.

The weak peaks at 2991 and 3020 cm^{-1} are contributed from the antisymmetric stretches of the ester methyl groups. The fitting results would be much worse if we set the strength of both peaks to zero for the PMMA/Ag interface. The 2991 cm^{-1} peak may also contain contributions from the asymmetric stretch of the α methyl groups. Here we deduce the possible tilt angle of the ester methyl groups at the PMMA/Ag interface by using the ratio of the nonlinear susceptibility tensor components $\chi_{yyz,s}$ and $\chi_{yyz,as}$.[16,25] Such a ratio is related to the orientation angle θ of ester methyl groups vs the surface normal through the following relation:

$$\left|\frac{\chi_{yyz,s}}{\chi_{yyz,as}}\right| = \left|\frac{\alpha_{ccc}[\cos\theta(1+r) - \cos^3\theta(1-r)]}{2\alpha_{caa}(\cos\theta - \cos^3\theta)}\right| \qquad (11)$$

where α_{ccc} and α_{caa} are hyperpolarizability components, r is the ratio of the two hyperpolarizability components and $r = \alpha_{aac}/\alpha_{ccc}$. Figure 7 shows the calculated $|\chi_{yyz,s}/\chi_{yyz,as}|$ value as a function of θ_0 for several different tilt angle distributions (0°, 10°, 20°, 30°, 34°, 40°) when a Gaussian distribution function is assumed. Since both the peaks are quite weak, and the ester methyl and α-methyl groups may contribute to the peak at 2991 cm^{-1}, only a semiquantitative discussion on the "possible" orientation range is given here. The upper limit considers that the antisymmetric stretches at 2991 cm^{-1} and at 3020 cm^{-1} of the ester methyl groups generate the same intensity. The lower limit considers that the peak at 2991 cm^{-1} is only from the

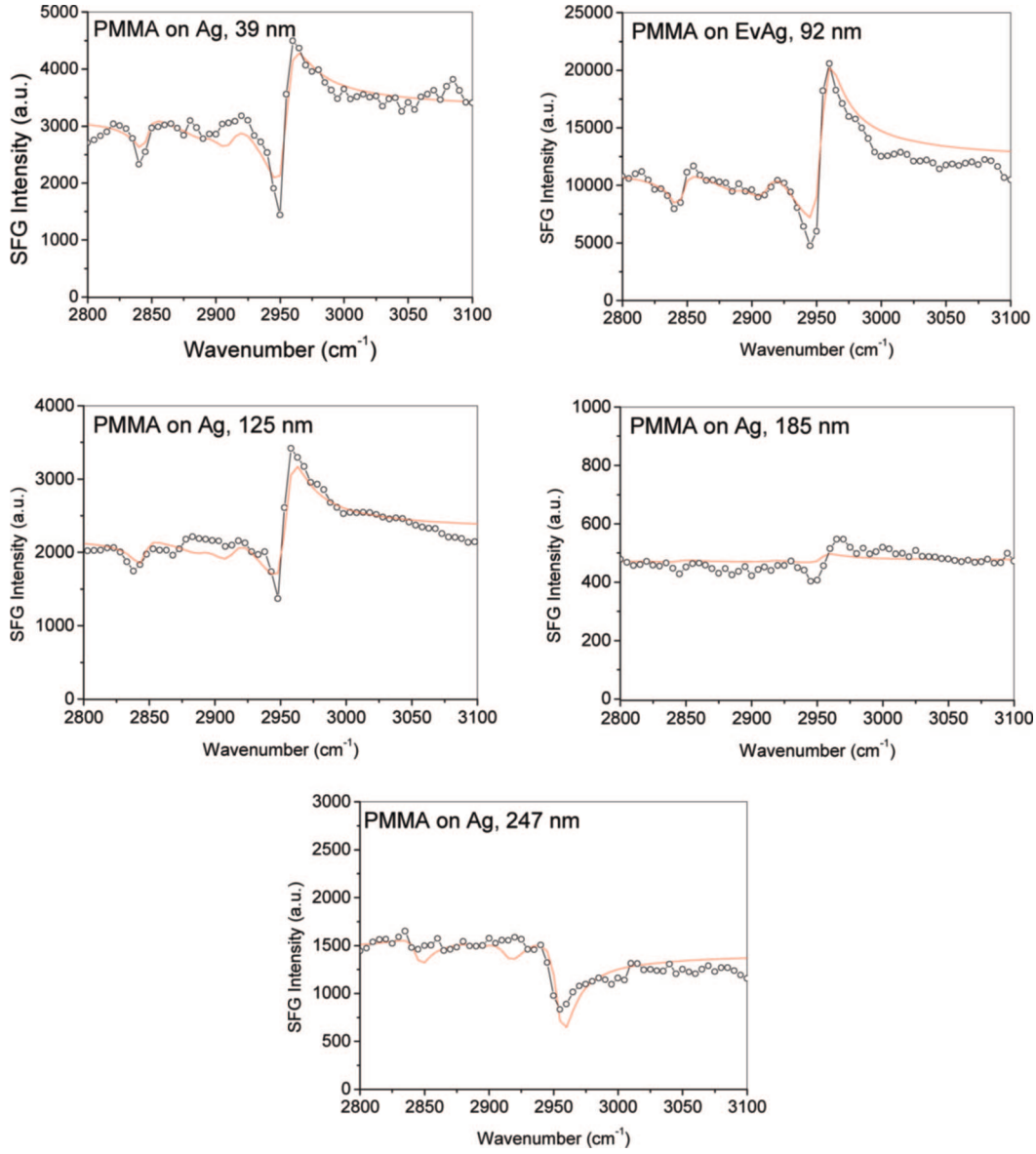

Figure 4. Best fit for the ssp SFG spectra of PMMA films with the contribution only from the PMMA/air interface.

ester methyl groups with no contribution from the α-methyl groups. In the latter case, the asymmetric stretching intensity of the ester methyl group is the sum of the intensity of the 2991 cm^{-1} and 3020 cm^{-1} peaks.

Considering the upper limit while the measured $|\chi_{yyz,s}/\chi_{yyz,as}|$ is 2.75, the possible orientation is between the two extremes of a tilt angle of 45° with a δ-distribution and a tilt angle of 90° with a distribution width of 40°. Considering the lower limit while the measured $|\chi_{yyz,s}/\chi_{yyz,as}|$ is 2.47, the possible orientation is between the two extremes of a tilt angle of 48° with a δ-distribution and a tilt angle of 90° with a distribution width of 34°. The possible tilt angles and the angle distributions should be inside the hatched areas shown in Figure 7. Nevertheless, the possible tilt angles of the ester methyl groups at the PMMA/Ag interface are larger than those at the PMMA/air interface. Therefore the ester methyl groups tilt more toward the surface at the PMMA/Ag interface comparing to those at the PMMA/air interface.

As we discussed in the previous publication,[12] the two ester methyl group asymmetric modes should have similar signal intensities, which means that the contribution of the α-methyl asymmetric stretch for the 2991 cm^{-1} peak should have a negative phase—then its symmetric stretch at ~2940 cm^{-1} should be positive. While the deduced 2940 cm^{-1} signal has a negative phase, thus we believe that it is not dominated by the contribution from the α-methyl symmetric stretch, but the symmetric stretch of the methylene groups. Therefore such methylene groups adopt a different absolute orientation comparing to the ester methyl groups.

When PMMA films with different thicknesses are deposited on the Ag substrates (e.g., 92 and 185 nm), their SFG signal intensities can differ by 2 orders of magnitudes (Figure 3). The signal intensity is contributed by many factors, such as the nonresonant background and the Fresnel coefficients in front of the resonant contribution terms as shown in eq 10. The origin of the nonresonant background is quite complicated. We found that the best fitting of various PMMA samples generated different values of χ_{NR}. In Equation 10, if χ_{NR} is substituted by $F_{yyz}^{interface}\chi'_{NR}$ and the nonresonant background is assumed only generated from the Ag substrate surface, χ'_{NR} is still varied when the film thickness is different, as shown in Table 2. This suggests that χ_{NR} is not only from the silver substrate.

5. Conclusion

This research developed a methodology to probe buried polymer/metal interfaces using SFG. The PMMA/Ag inter-

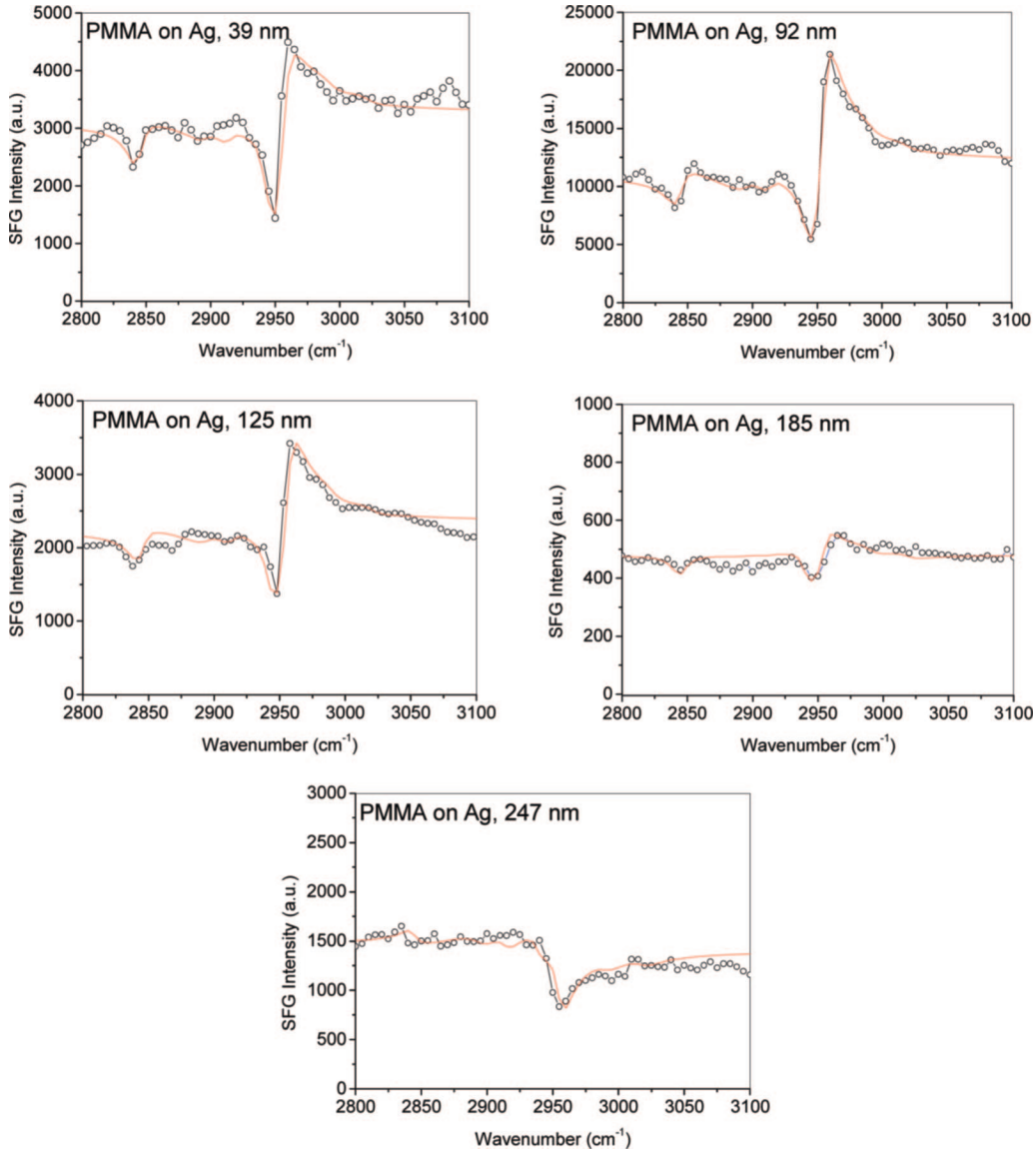

Figure 5. Best fit for the ssp SFG spectra of PMMA films with the contributions both from the PMMA/air interface and the PMMA/Ag interface.

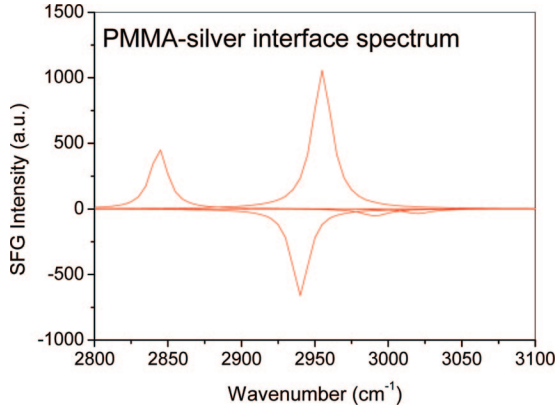

Figure 6. Fitted spectrum for the PMMA/Ag interface.

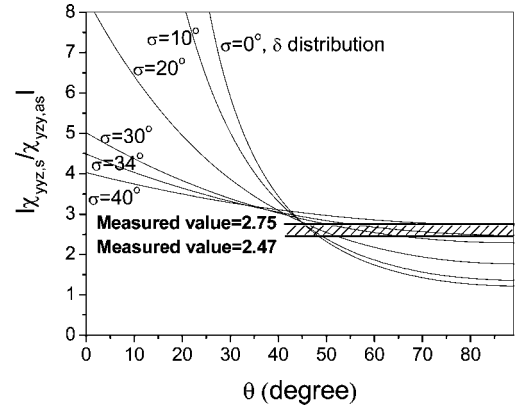

Figure 7. Calculated values of $|\chi_{yyz,s}/\chi_{yyz,as}|$ as a function of the tilting angle θ_0 and angle distribution.

face was used as a model to develop this methodology. SFG spectra were collected from the PMMA films with different thicknesses on Ag substrates. Such spectra were successfully fitted using the interferences between the signals from the PMMA/air interface, the PMMA/Ag interface, and the nonresonant background, from which the SFG signal contributed from the PMMA/Ag buried interface can be deduced. Such SFG signals provide understanding on molecular structural information of the buried polymer/metal interface.

It has been shown that the PMMA structure at the PMMA/Ag interface is different from the PMMA surface in air. For

Table 2. Fitting Results for χ_{NR} and χ'_{NR}

thickness (nm)	39	92	125	185	247
χ_{NR}	57	108	48	22	38
χ'_{NR}	384	355	348	304	243

the PMMA surface in air, ester methyl groups dominate the surface, with an ordered orientation pointing toward the surface normal. At the PMMA/Ag interface, in addition to the ester methyl groups, methylene and α methyl groups also present at the interface. The ester methyl groups at the PMMA/Ag interface is deduced to point away from the Ag substrate with a larger tilt angle, tilting more toward the interface.

This research demonstrates that it is feasible to probe molecular structures of buried polymer/metal interfaces *in situ* using SFG. We believe that continued success in the research in this direction will develop SFG into a powerful and nondisruptive tool to study polymer/metal interfaces, providing important information to optimize interfacial structures to enhance the properties (e.g., adhesion) of polymer/metal interfaces. Currently further SFG studies on many other polymers at the polymer/metal interfaces are being carried out and molecular dynamics simulations are being used in the research to confirm SFG results.

Acknowledgment. This work is supported by NSF (CHE-0449469), Dow Corning Corporation, University of Michigan, and Nanjing University. We want to thank Lurie Nanofabrication Facility for the help in sample preparation. We want to thank Dr. Jie Wang and Dr. Zoltan Paszti for their excellent suggestions and Mr. Alex D. Martin for his help in this research.

Supporting Information Available: Text giving more details regarding the Fresnel coefficient calculations and optical constants used, including a figure showing a schmenatic of the sample and tables giving the optical constants used to obtain the Fresnel coefficients and fitting results for the phase difference. This information is available free of charge via the Internet at http://pubs.acs.org.

References and Notes

(1) Feast, W. J.; Munro, H. S.; Richards, R. W. *Polymer Surfaces and Interfaces II*; John Wiley and Sons: New York, 1992.
(2) Park, G. S.; Lee, H. Y. *J. Mater. Sci.* **2002**, *37*, 4247–4257.
(3) Lee, H.-Y.; Park, Y.-B.; Jeon, I.; Kim, Y.-H.; Chang, Y.-K. *Mater. Sci. Eng.* **2005**, *A405*, 50–64.
(4) Chen, Z.; Shen, Y. R.; Somorjai, G. A. *Annu. Rev. Phys. Chem.* **2002**, *53*, 437–465.
(5) Zhang, D.; Ward, R. S.; Shen, Y. R.; Somorjai, G. A. *J. Phys. Chem. B* **1997**, *101*, 9060–9064.
(6) Opdahl, A.; Somorjai, G. A. *Langmuir* **2002**, *18*, 9409–9412.
(7) Ophahl, A.; Phillips, R. A.; Somorjai, G. A. *Macromolecules* **2002**, *35*, 4387–4396.
(8) Wei, X.; Zhuang, X.; Hong, S.-C.; Goto, T.; Shen, Y. R. *Phys. Rev. Lett.* **1999**, *82*, 4256–4259.
(9) Wei, X.; Hong, S.-C.; Zhuang, X.; Goto, T.; Shen, Y. R. *Phys. Rev. E* **2000**, *62*, 5160–5172.
(10) Kim, D.; Oh-e, M.; Shen, Y. R. *Macromolecules* **2001**, *34*, 9125–9129.
(11) Hong, S.-C.; Zhang, C.; Shen, Y. R. *Appl. Phys. Lett.* **2003**, *82*, 3068–3070.
(12) Wang, J.; Chen, C.; Buck, S. M.; Chen, Z. *J. Phys. Chem. B* **2001**, *105*, 12118–12125.
(13) Wang, J.; Woodcock, S. E.; Buck, S. M.; Chen, C.; Chen, Z. *J. Am. Chem. Soc.* **2001**, *123*, 9470–9471.
(14) Wang, J.; Paszti, Z.; Even, M. A.; Chen, Z. *J. Am. Chem. Soc.* **2002**, *124*, 7016–7023.
(15) Chen, C.; Wang, J.; Even, M. A.; Chen, Z. *Macromolecules* **2002**, *35*, 8093–8097.
(16) Chen, C.; Wang, J.; Chen, Z. *Langmuir* **2004**, *20*, 10186–10193.
(17) Clarke, M. L.; Wang, J.; Chen, Z. *Anal. Chem.* **2003**, *75*, 3275–3280.
(18) Chen, C.; Wang, J.; Loch, C. L.; Ahn, D.; Chen, Z. *J. Am. Chem. Soc.* **2004**, *126*, 1174–1179.
(19) Loch, C. L.; Ahn, D.; Vazquez, A. V.; Chen, Z. *J. Colloid Interface Sci.* **2007**, *308*, 170–175.
(20) Chen, C.; Loch, C. L.; Wang, J.; Chen, Z. *J. Phys. Chem. B* **2003**, *107*, 10440–1045.
(21) Loch, C. L.; Ahn, D.; Chen, Z. *J. Phys. Chem. B* **2006**, *110*, 914–918.
(22) Loch, C. L.; Ahn, D.; Chen, C.; Wang, J.; Chen, Z. *Langmuir* **2004**, *20*, 5467–5473.
(23) Johnson, W. C.; Wang, J.; Chen, Z. *J. Phys. Chem. B* **2005**, *109*, 6280–6286.
(24) Even, M. A.; Chen, C.; Wang, J.; Chen, Z. *Macromolecules* **2006**, *39*, 9396–9401.
(25) Gautam, K. S.; Dhinojwala, A. *Macromolecules* **2001**, *34*, 1137–1139.
(26) Rangwalla, H.; Dhinojwala, A. *J. Adhes.* **2004**, *80*, 37–59.
(27) Zhang, D.; Dougal, S. M.; Yeganeh, M. S. *Langmuir* **2000**, *16*, 4528–4532.
(28) Briggman, K. A.; Stephenson, J. C.; Wallace, W. E.; Richter, L. J. *J. Phys. Chem. B* **2001**, *105*, 2785–2791.
(29) Wilson, P. T.; Briggman, K. A.; Wallace, W. E.; Stephenson, J. C.; Richter, L. J. *Appl. Phys. Lett.* **2002**, *80*, 3084–3086.
(30) Wilson, P. T.; Richter, L. J.; Wallace, W. E.; Briggman, K. A.; Stephenson, J. C. *Chem. Phys. Lett.* **2002**, *363*, 161–168.
(31) Morita, S.; Ye, S.; Li, G.; Osawa, M. *Vibr. Spectrosc.* **2004**, *35*, 15–19.
(32) Ye, S.; Morita, S.; Li, G.; Noda, H.; Tanaka, M.; Uosaki, K.; Osawa, M. *Macromolecules* **2003**, *36*, 5694–5703.
(33) Ye, H. K.; Gu, Z. Y.; Gracias, D. H. *Langmuir* **2006**, *22*, 1863–1868.
(34) Jayathilake, H. D.; Zhu, M. H.; Rosenblatt, C.; Bordenyuk, A. N.; Weeraman, C.; Benderskii, A. V. *J. Chem. Phys.* **2006**, *125*, 064706.
(35) Li, Q. F.; Hua, R.; Cheah, I. J.; Chou, K. C. *J. Phys. Chem. B* **2008**, *112*, 694–697.
(36) Li, Q.; Hua, R.; Chou, K. C. *J. Phys. Chem. B* **2008**, *112*, 2315–2318.
(37) Liu, Y.; Messmer, M. C. *J. Phys. Chem. B* **2003**, *107*, 9774–9779.
(38) Miyamae, T.; Nozoye, H. *Surf. Sci.* **2003**, *532*, 1045–1050.
(39) Park, J. B.; Lakes, R. S. *Biomaterials: an Introduction*;Plenum Press: New York, 1992.
(40) Stroeve, P.; Franses, E. I. *Molecular Engineering of Ultrathin Film*; Elsevier: London, 1987.
(41) Roberts, G. G. *Langmuir-Blodgett Films*; Plenum Press: New York, 1990.
(42) Ulman, A. *An Introduction to Ultrathin Organic Films. From Langmuir-Blodgett to Self-Assembly*; Academic Press: New York, 1991.
(43) Kuan, S. W.; Frank, C. W.; Lee, Y. H.; Eimori, T.; Allee, D. R.; Pease, R. F. W.; Browning, R. J. *Vac. Sci. Technol. B.* **1989**, *7*, 1745–1750.
(44) Wu, S. *Polymer Interface and Adhesion*; Marcel Dekker: New York, 1982.
(45) Kwok, D. Y.; Leung, A.; Lam, C. N. C.; Li, A.; Wu, R.; Neumann, A. W. *J. Colloid Interface Sci.* **1998**, *206*, 44–51.
(46) Inoue, C.; Kaneda, Y.; Aida, M.; Endo, K. *Polym. J.* **1995**, *27*, 300–309.
(47) Cross, T.; Lippitz, A.; Unger, W.; Woll, C.; Hahner, G.; Braun, W. *Appl. Surf. Sci.* **1993**, *68*, 291–298.
(48) Leeson, A. M.; Alexander, M. R.; Short, R. D.; Briggs, D.; Hearn, M. J. *Surf. Interface Anal.* **1997**, *25*, 261–274.
(49) Briggs, D.; Fletcher, I. W.; Goncalves, N. M. *Surf. Interface Anal.* **2000**, *29*, 303–309.
(50) Leggett, G. J.; Vickerman, J. C. *Appl. Surf. Sci.* **1992**, *55*, 105–115.
(51) Deimel, M.; Rulle, H.; Liebing, V.; Benninghoven, A. *Appl. Surf. Sci.* **1998**, *134*, 271–274.
(52) Pignataro, B.; Fragala, M. E.; Puglisi, O. *Nucl. Instrum. Methods Phys. Rev. B* **1997**, *131*, 141–148.
(53) Wilk, D.; Johannsmann, D.; Stanners, C.; Shen, Y. R. *Phys. Rev. B* **1995**, *51*, 10057–10067.
(54) Ye, H.; Abu-Akeel, A.; Huang, J.; Katz, H. E.; Gracias, D. H. *J. Am. Chem. Soc.* **2006**, *128*, 6528–6529.
(55) Ye, H.; Huang, J.; Park, J.-R.; Katz, H. E.; Gracias, D. H. *J. Phys. Chem. C.* **2007**, *111*, 13250–13255.
(56) Shen, Y. R. *The Principles of Nonlinear Optics*; Wiley: New York, 1984.
(57) Shen, Y. R. *Annu. Rev. Phys. Chem.* **1989**, *40*, 327–350.
(58) Guyot-Sionnest, P.; Hunt, J. H.; Shen, Y. R. *Phys. Rev. Lett.* **1987**, *59*, 1597–1600.
(59) Miranda, P. B.; Shen, Y. R. *J. Phys. Chem. B* **1999**, *103*, 3292–3307.
(60) Bain, C. D. *J. Chem. Soc. Fraday Trans.* **1995**, *91*, 1281–1296.
(61) Eisenthal, K. B. *Chem. Rev.* **1996**, *96*, 1343–1360.
(62) Chen, Z.; Gracias, D. H.; Somorjai, G. A. *Appl. Phys. B: Lasers Opt.* **1999**, *68*, 549–557.
(63) Shultz, M. J.; Schnitzer, C.; Simonelli, D.; Baldelli, S. *Int. Rev. Phys. Chem.* **2000**, *19*, 123–153.
(64) Kim, J.; Cremer, P. S. *J. Am. Chem. Soc.* **2000**, *122*, 12371–12372.
(65) Chen, Z. *Polym. Int.* **2006**, *65*, 577–587.

(66) Zhuang, X.; Miranda, P. B.; Kim, D.; Shen, Y. R. *Phys. Rev. B* **1999**, *59*, 12632–12640.
(67) Nagai, H. *J. Appl. Polym. Sci.* **1963**, *7*, 1697–1714.
(68) Dirlikov, S. K.; Koenig, J. L. *Appl. Spectrosc.* **1979**, *33*, 555–561.
(69) Schneider, B.; Stokr, J.; Schmidt, P.; Mihailov, M.; Dirlikov, S.; Peeva, N. *Polymer* **1979**, *20*, 705–712.
(70) Lipschitz, I. *Polym.-Plast. Technol. Eng.* **1982**, *19*, 53–102.
(71) Dybal, J.; Krimm, S. *Macromolecules* **1990**, *23*, 1301–1308.
(72) Feller, M. B.; Chen, W.; Shen, Y. R. *Phys. Rev. A* **1991**, *43*, 6778–6792.
(73) Ward, R. N.; Davies, P. B.; Bain, C. D. *J. Phys. Chem.* **1993**, *97*, 7141–7143.

MA801680F